

Fig. S1. PC influences body weight and hematological parameters in naturally aged mice. (A) Body weight measurements were taken at baseline and 45 days post-gavage with saline or PC. (B) Percentage of neutrophils. (C) Percentage of monocytes. (D) Percentage of abnormal lymphocytes. (E) Platelet count. (F) Red blood cell count. (G) Lymphocyte ratio. For (A), whiskers indicate min to max. For (B-G), data are presented as mean ± SD. Data were processed by one-way ANOVA followed by Tukey multiple-comparison post hoc tests. P < 0.05 indicates significant differences between treatments. The number of mice in each group is indicated in parentheses.

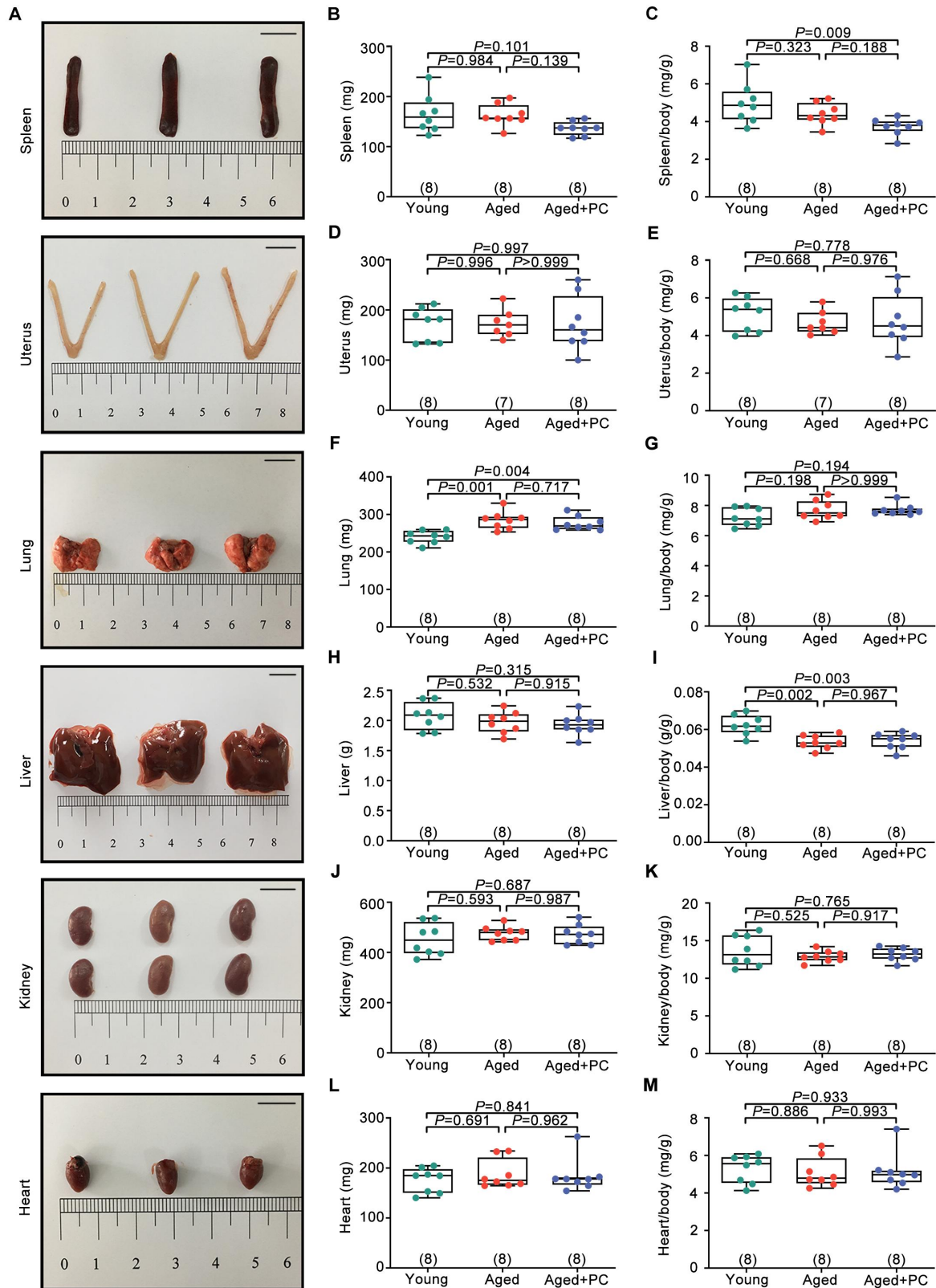


Fig. S2. PC has no effect on organ weight and relative organ weight in naturally aged mice. (A) Organ views. No significant morphological differences were observed between treatments. Scale bar = 1 cm. (B) Spleen weight. (C) Relative spleen weight. (D) Uterus weight. (E) Relative uterus weight. (F) Lung weight. (G) Relative lung weight. (H) Liver weight. (I) Relative liver weight. (J) Kidney

14 weight. (K) Relative kidney weight. (L) Heart weight. (M) Relative heart weight. Whiskers indicate
15 min to max. Data are processed by one-way ANOVA followed by Tukey multiple-comparison post
16 hoc tests. $P < 0.05$ indicates significant differences between treatments. The number of mice in each
17 group is indicated in parentheses.

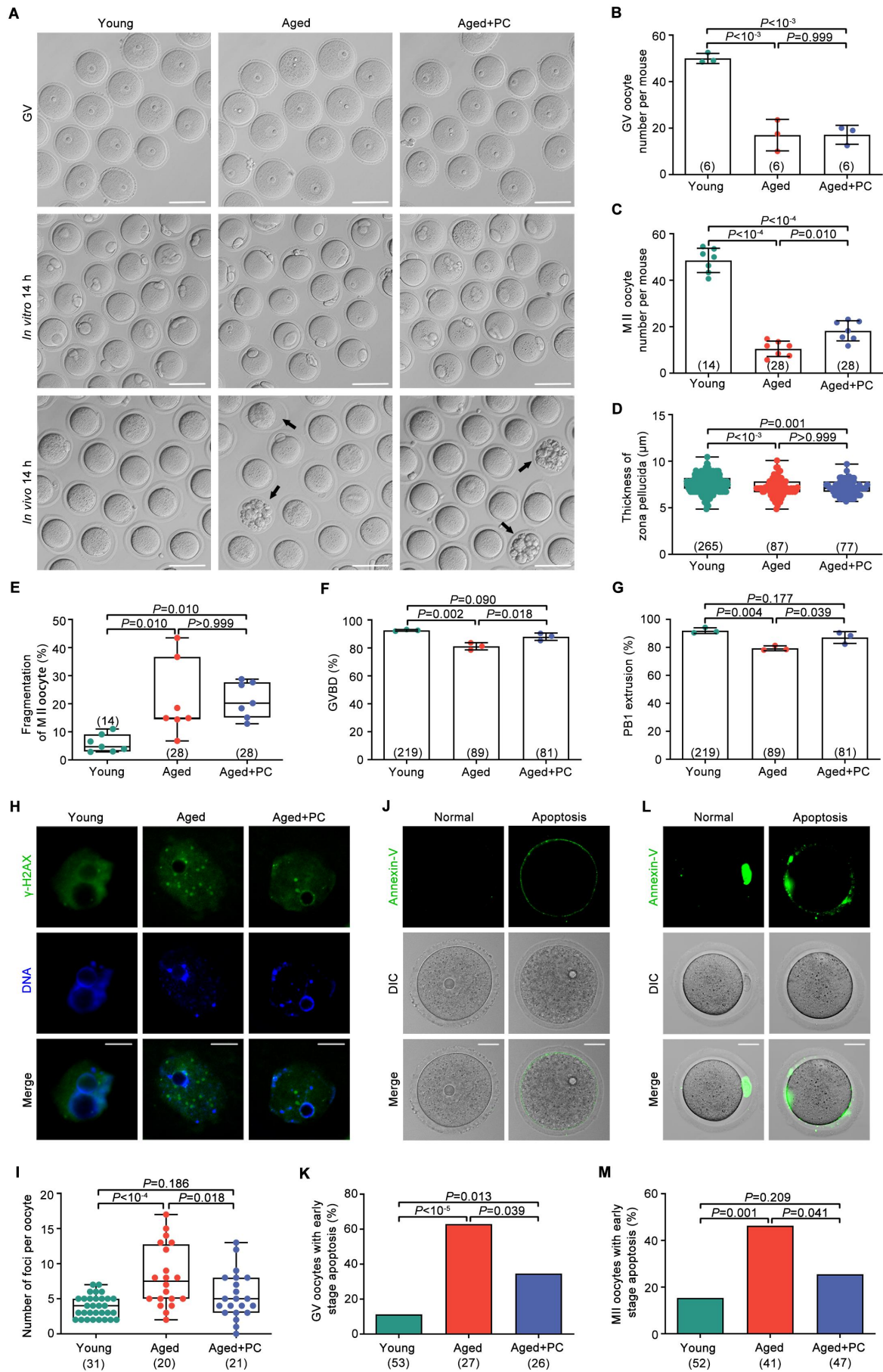


Fig. S3. PC rescues oocyte quality and reduces early apoptosis in naturally aged mice. (A) Oocyte morphology was assessed at the GV and MII stages *in vitro* or *in vivo*. Morphologically abnormal oocytes are indicated by black arrow. Scale = 100 μ m. (B) Number of GV oocytes. (C) Number of MII oocytes. (D) Zona pellucida thickness of GV oocytes. (E) Percentage of MII oocytes with fragmentation morphologies. (F) Percentage of oocytes undergoing GVBD. (G) Percentage of oocytes undergoing PB1 extrusion. (H) Diagram of DNA double-strand breaks in GV oocytes. Scale bar = 20 μ m. (I) Number of DNA double-stranded breaks in GV oocytes. (J) Representative images of normal and early apoptotic GV oocytes. Early apoptosis is labeled by green fluorescence on the oocyte membrane. Scale bar = 20 μ m. (K) Percentage of apoptosis in GV oocytes. (L) Representative images of normal and early apoptotic MII oocytes. Early apoptosis is labeled by green fluorescence on the oocyte membrane. Scale bar = 20 μ m. (M) Percentage of apoptotic MII oocytes. For (B, C, F, G), data are presented as mean \pm SD. For (D, E, I), whiskers indicate min to max. Data were processed by one-way ANOVA followed by Tukey multiple-comparison post hoc tests for (B-G, I), and chi-squared tests for (K, M). $P < 0.05$ indicates significant differences between treatments. The number of mice or oocytes in each group is indicated in parentheses.

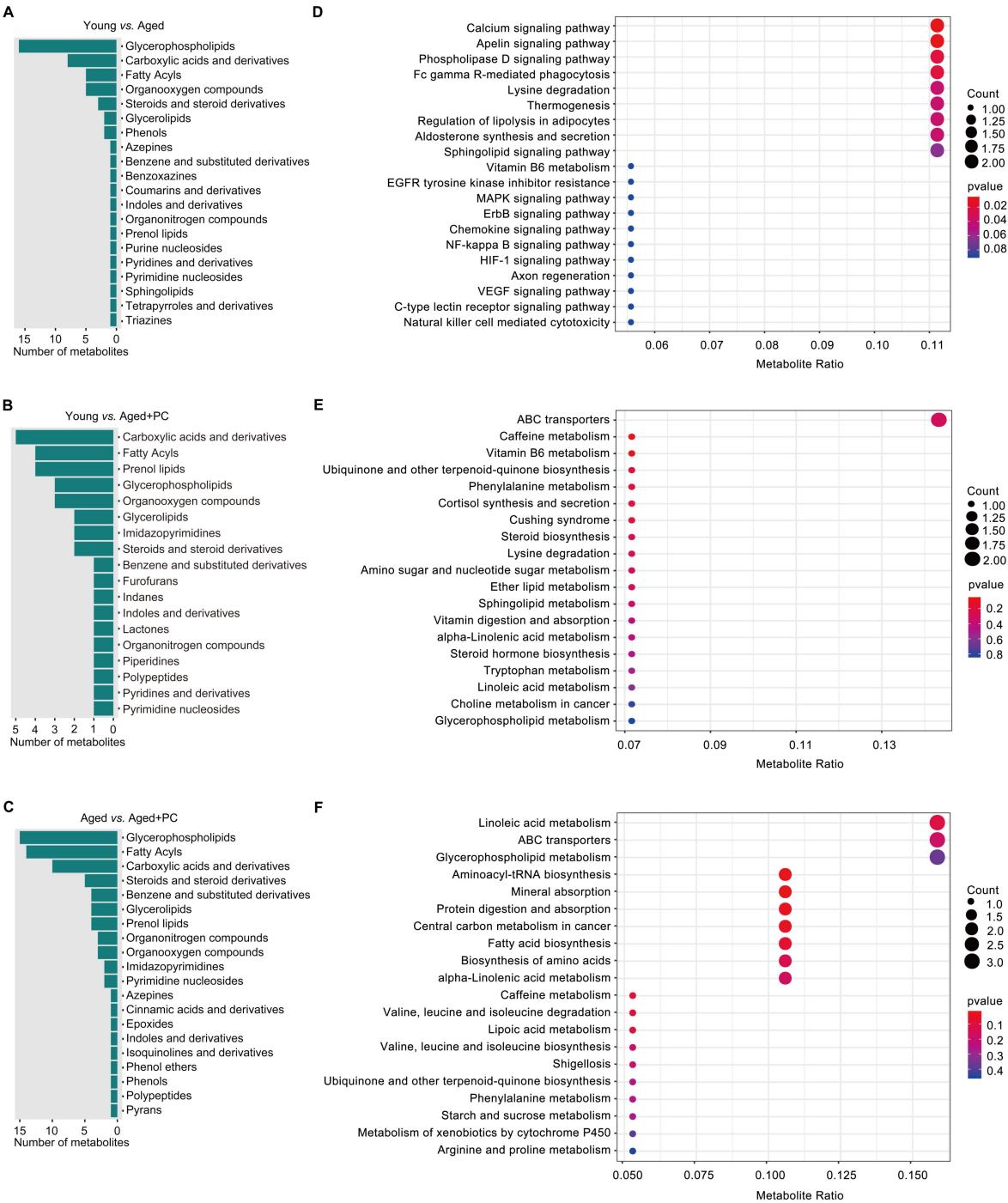


Fig. S4. HMDB classification and KEGG pathway enrichment analysis of differential metabolites. (A) HMDB classification of differential metabolites between the Young and Aged groups. (B) HMDB classification of differential metabolites between the Young and Aged+PC groups. (C) HMDB classification of differential metabolites between the Aged and Aged+PC groups. (D) KEGG pathway enrichment analysis of differential metabolites between the Young and Aged groups. (E) KEGG pathway enrichment analysis of differential metabolites between the Young and Aged+PC groups. (F) KEGG pathway enrichment analysis of differential metabolites between the Aged and Aged+PC groups. Five mice per group were used for metabolomics analysis.

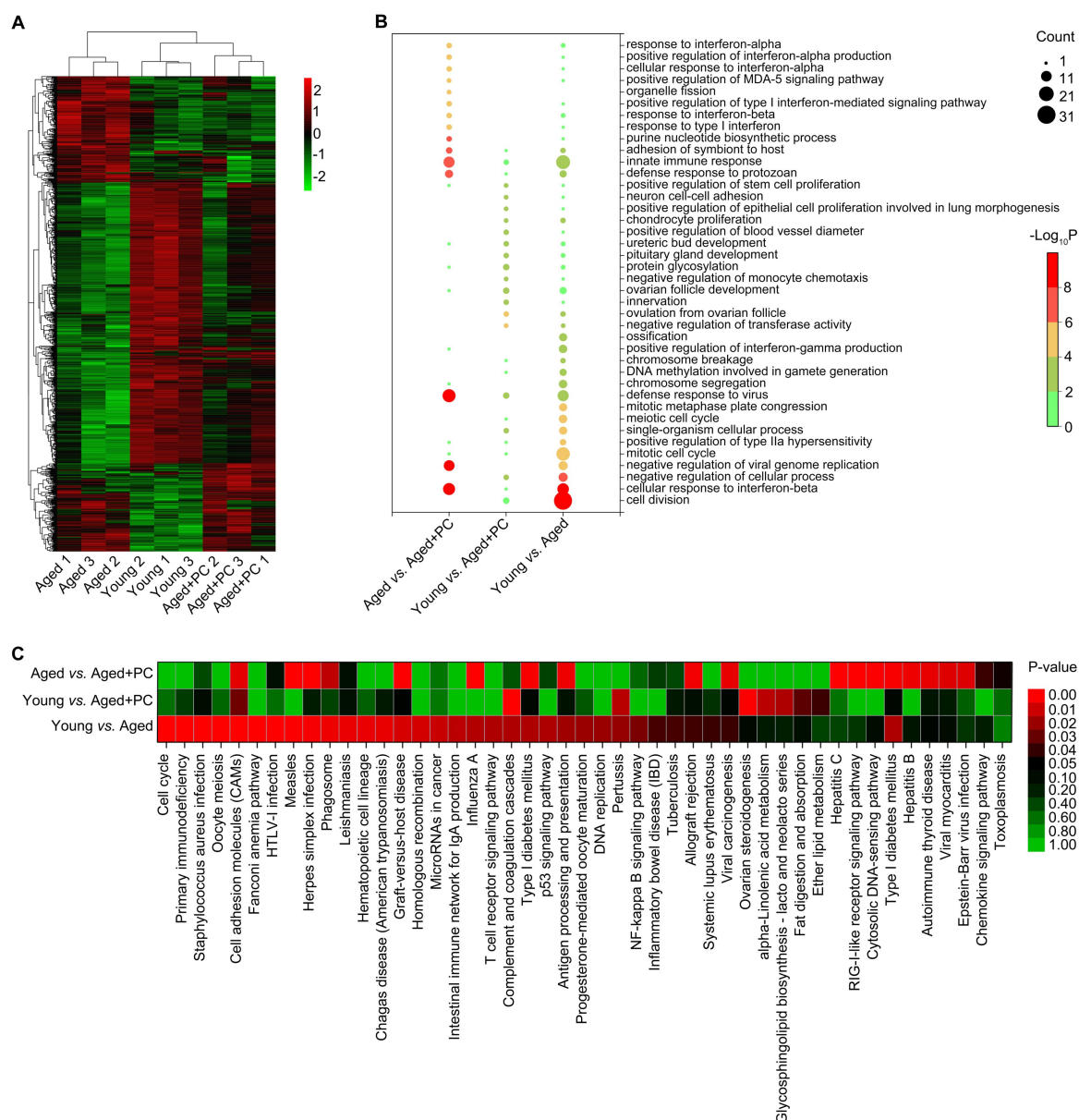


Fig. S5. Gene Ontology and KEGG pathway enrichment analysis of differentially expressed genes (DEGs). (A) Cluster heat map of DEGs. (B) Gene Ontology enrichment analysis of the DEGs in biological process. (C) Heatmap of differential KEGG pathways. **Three mice per group were used for RNA sequencing.**

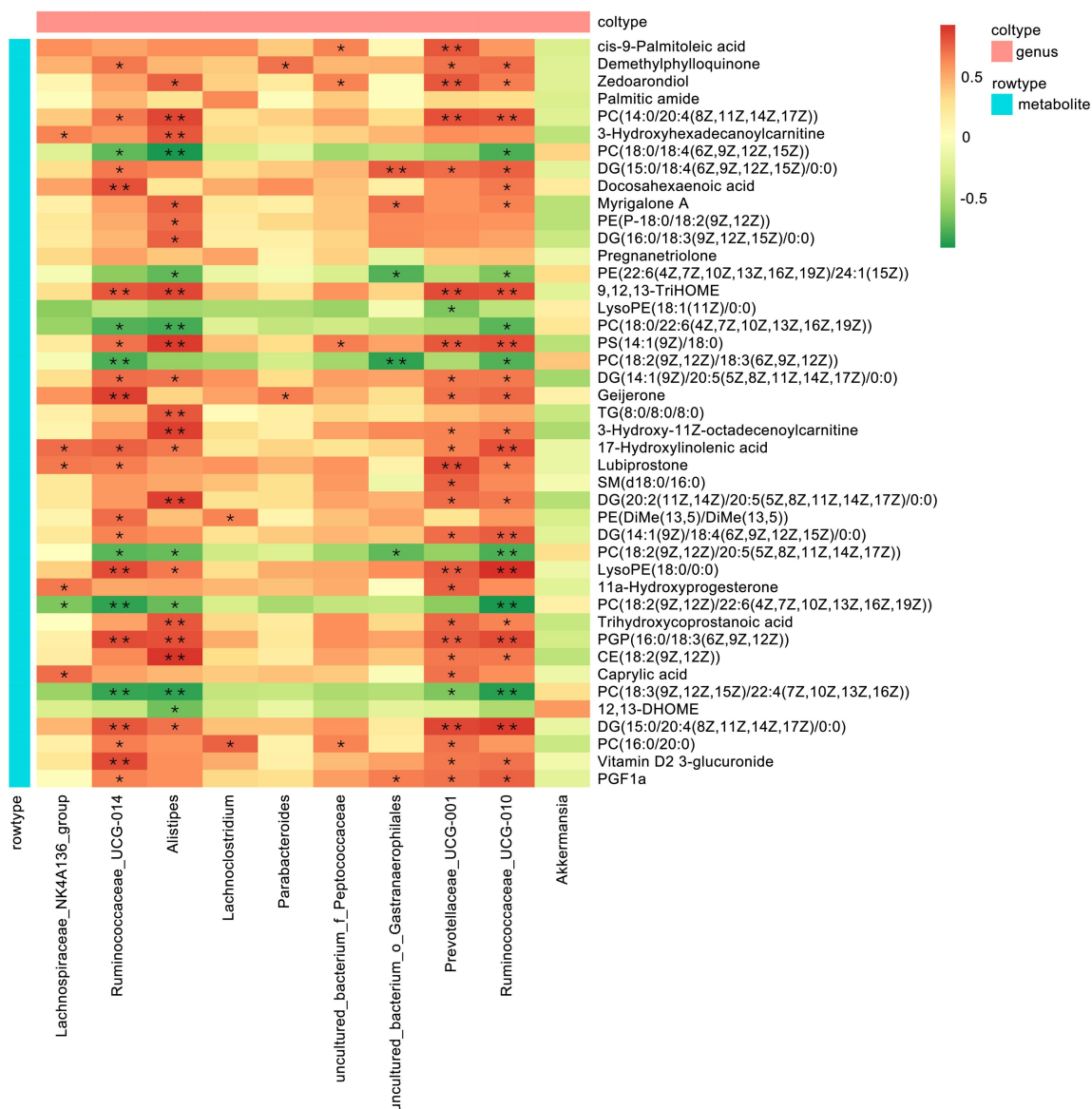


Fig. S6. Correlation heatmap of gut microbes and differential lipid metabolites in serum between the Aged and Aged+PC groups. * $P < 0.05$ indicates significant correlation.



Fig. S7. Correlation heatmap of differential lipid metabolites in serum and interferon-related genes of differentially expressed genes (DEGs) in ovary between the Aged and Aged+PC groups.

**P*<0.05 indicates significant correlation.

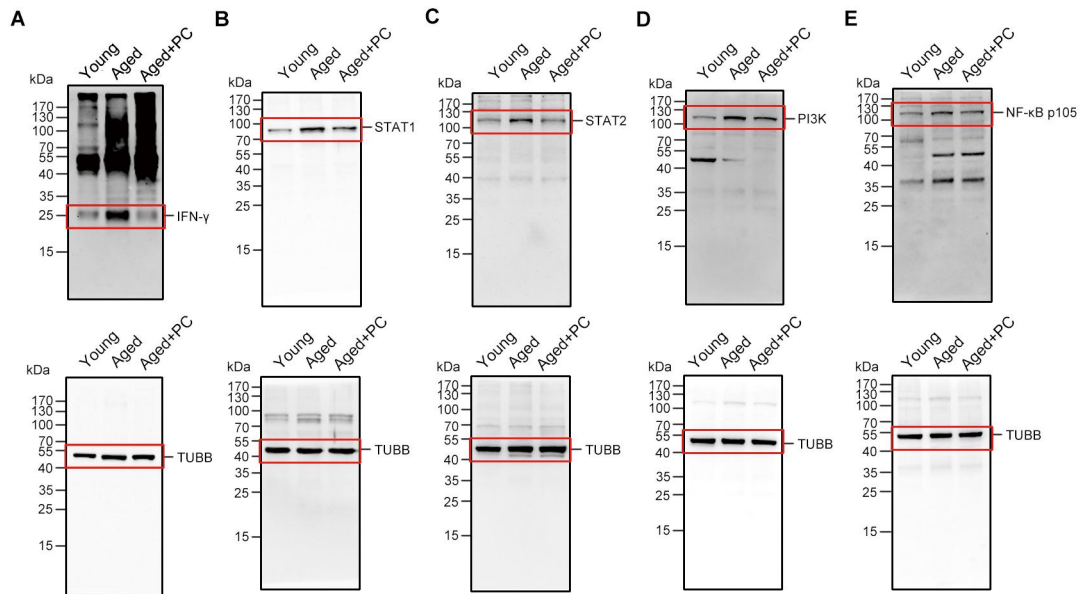


Fig. S8. Raw western blot data. (A) Original western blot results for Fig. 6H. (B) Original western blot results for Fig. 6J. (C) Original western blot results for Fig. 6L. (D) Original western blot results for Fig. 6N. (E) Original western blot results for Fig. 6P.

Table S1 Sequences of primers for qRT-PCR

Gene	Forward	Reverse
<i>Gapdh</i>	CGTCCCGTAGACAAAATGGT	TTGATGGCAACAATCTCCAC
<i>Gm4951</i>	TGGGCTACTGAGCTTCTTCTT	GCCCTCACCTGATCTACCTG
<i>Ifi203</i>	ACCATCCAGCAGTTCCTCAAA	TTTGGTACAGTTCCTCTCCTTGG
<i>Ifi44</i>	AACTGACTGCTCGCAATAATGT	GTAACACAGCAATGCCTCTTGT
<i>Ifit3</i>	TTCCCGGTTGACCTCACTCA	CTGAACTGCTCAGCCCAC
<i>Ifnar1</i>	ACACTGCCCATTGACTCTCC	TTGGGTGCTACCCTCAGC
<i>Ifnar2</i>	CTTCGTGTTTGGTAGTGATGGT	GGGGATGATTTCCAGCCGA
<i>Ifngr1</i>	TACAGGTAAAGGTGTATTCGGGT	ACCGTGCATAGTCAGATTCTTTT
<i>Ifngr2</i>	TCCTCGCCAGACTCGTTTTTC	GTCTTGGGTCATTGCTGGAAG
<i>Igtp</i>	CGCCTCATCAGCCCGTGGTCTAA	TGCCATTGCCAGAGTCCCCAGTC
<i>Isg15</i>	CAATGGCCTGGGACCTAA	CGGCACACCAATCTTCTG
<i>Stat1</i>	TCACAGTGGTTCGAGCTTCAG	GCAAACGAGACATCATAGGCA
<i>Stat2</i>	TTCCGCTGTTGCTATCTT	ATCTCCCACTGCGCCATT
<i>Zbp1</i>	AAGAGTCCCCTGCGATTATTTG	TCTGGATGGCGTTTGAATTGG

Table S2 The relative abundance of gut microbes between groups of mice at the genus level

genus	Young	Aged	Aged+PC
Alistipes	0.00875 ± 0.00299 ^a	0.05633 ± 0.01948 ^b	0.01387 ± 0.00499 ^a
Ruminococcaceae_UCG-014	0.00195 ± 0.00087 ^a	0.01810 ± 0.00636 ^b	0.00162 ± 0.00042 ^a
Candidatus_Saccharimonas	0.00428 ± 0.00122 ^a	0.01377 ± 0.00314 ^b	0.00635 ± 0.00175 ^a
uncultured_bacterium_f_Desulfovibrionaceae	0.10170 ± 0.02028 ^a	0.02219 ± 0.00815 ^b	0.05036 ± 0.03479 ^{ab}
uncultured_bacterium_f_Lachnospiraceae	0.04398 ± 0.01426 ^a	0.12882 ± 0.03262 ^b	0.13756 ± 0.07217 ^{ab}
Enterorhabdus	0.00013 ± 0.00008 ^a	0.00124 ± 0.00053 ^b	0.00199 ± 0.00117 ^{ab}
Paraprevotella	0.00228 ± 0.00113 ^a	0.00000 ± 0.00000 ^b	0.00055 ± 0.00041 ^{ab}
Bilophila	0.00049 ± 0.00021 ^a	0.00376 ± 0.00162 ^b	0.00514 ± 0.00439 ^{ab}
Lachnospiraceae_UCG-006	0.00075 ± 0.00018 ^a	0.00565 ± 0.00250 ^b	0.00443 ± 0.00202 ^{ab}
Ruminococcaceae_UCG-004	0.00031 ± 0.00013 ^a	0.00111 ± 0.00039 ^b	0.00082 ± 0.00032 ^{ab}
Parasutterella	0.00753 ± 0.00324 ^a	0.00123 ± 0.00044 ^b	0.00827 ± 0.00426 ^{ab}
Lactobacillus	0.01064 ± 0.00263 ^a	0.04872 ± 0.01463 ^b	0.05187 ± 0.01871 ^b
Anaerotruncus	0.00773 ± 0.00295 ^a	0.00092 ± 0.00067 ^b	0.00000 ± 0.00000 ^b
Lachnospiraceae_NK4A136_group	0.12035 ± 0.03162 ^{ab}	0.22365 ± 0.05263 ^a	0.07508 ± 0.03558 ^b
Gordonibacter	0.00040 ± 0.00024 ^{ab}	0.00009 ± 0.00009 ^a	0.00000 ± 0.00000 ^b
Ruminococcaceae_UCG-013	0.00027 ± 0.00011 ^a	0.00148 ± 0.00075 ^{ab}	0.00217 ± 0.00053 ^b
Ruminiclostridium_9	0.00425 ± 0.00096 ^a	0.01021 ± 0.00312 ^{ab}	0.00814 ± 0.00174 ^b
Ruminiclostridium_5	0.00009 ± 0.00009 ^a	0.00091 ± 0.00045 ^{ab}	0.00083 ± 0.00038 ^b
[Eubacterium]_xylanophilum_group	0.00066 ± 0.00035 ^a	0.00036 ± 0.00029 ^{ab}	0.00000 ± 0.00000 ^b
Alloprevotella	0.02683 ± 0.01076 ^a	0.00785 ± 0.00360 ^{ab}	0.00612 ± 0.00229 ^b

Data are represented as mean ± SEM and statistical comparisons were made using *t*-tests by using Metastats. Without a common letter means statistically significant differences between treatments ($P < 0.05$). Six mice for used for each treatment.

Table S3 GSEA analysis of IFN-related GO items

Description	Young group vs. Aged group				Young group vs. Aged+PC group				Aged group vs. Aged+PC group			
	setSize	NES	pvalue	qvalue	setSize	NES	pvalue	qvalue	setSize	NES	pvalue	qvalue
response to IFN-gamma	17	1.718	0.013	0.126	17	-0.581	0.956	0.907	17	-2.150	0.002	0.078
cellular response to IFN-alpha	12	1.764	0.008	0.105	12	0.698	0.867	0.890	12	-1.996	0.002	0.078
positive regulation of type I IFN-mediated signaling pathway	11	1.854	0.004	0.080	11	-1.737	0.009	0.146	11	-2.156	0.002	0.078
positive regulation of IFN-beta production	19	1.523	0.039	0.241	19	-0.853	0.680	0.828	19	-1.988	0.002	0.078
cellular response to IFN-beta	49	2.705	0.003	0.071	46	-1.017	0.427	0.730	49	-2.950	0.002	0.078
cellular response to IFN-gamma	56	2.138	0.003	0.071	52	0.891	0.669	0.824	57	-2.297	0.002	0.078
positive regulation of IFN-gamma production	31	1.886	0.002	0.071	31	1.207	0.215	0.586	30	-1.740	0.006	0.104
negative regulation of IFN-gamma production	14	1.744	0.009	0.106	14	1.471	0.056	0.343	16	-1.480	0.058	0.325